Fungal Genetics and Biology 123 (2019) 1–13

Contents lists available at ScienceDirect

Fungal Genetics and Biology

journal homepage: www.elsevier.com/locate/yfgbi

Fusarium graminearum KP4-like proteins possess root growth-inhibiting activity against wheat and potentially contribute to fungal virulence in seedling rot☆

Shunwen Lu*, Justin D. Faris

US Department of Agriculture, Agricultural Research Service, Cereal Crops Research Unit, Fargo, ND 58102-2765, USA

ARTICLE INFO

Keywords:
Fungal pathogenicity
Fusarium root rot
Host-selective toxins
Seedling disease
Wheat-pathogen interactions

ABSTRACT

The virally encoded KP4 killer toxin protein was first identified from *Ustilago maydis* (Um), and its homologues are present in diverse fungi and in one species of moss. No KP4-like (KP4L) proteins have been functionally characterized. Here, we report the identification and functional analysis of four KP4L proteins from *Fusarium graminearum* (Fg), the primary causal pathogen of Fusarium head blight (FHB), which is also known to associate with seedling rot of wheat. The four FgKP4L proteins (FgKP4L-1, -2, -3 and -4) are encoded by small open reading frames (378–825 bp) located on chromosome 1 with the *FgKP4L-1*, *-2* and *-3* genes clustering together. Sequence analysis indicated that FgKP4L proteins have conserved domains predicted to form a three-dimensional alpha/beta-sandwich structure as first reported for UmKP4, with FgKP4L-4 featuring double Kp4 domains. Further analyses revealed that the *FgKP4L* genes are expressed *in vitro* under certain stress conditions, and all up-regulated during FHB and/or seedling rot development, the recombinant FgKP4L-2 protein does not induce cell death in wheat leaves or spikelets, but inhibits root growth of young seedlings, and the elimination of the *FgKP4L-1/-2/-3* gene cluster from the fungal genome results in reduced virulence in seedling rot but not in FHB. Database searches revealed KP4L proteins from ~80 fungal species with more than half from human/animal pathogens. Phylogenetic analysis suggested that UmKP4 and the moss KP4L proteins are closely related to those from a zygomycete and *Aspergillus*, respectively, implying cross-kingdom horizontal gene transfer.

1. Introduction

Fusarium graminearum is the primary causal pathogen of Fusarium head blight (FHB), one of the most devastating diseases of wheat and barley worldwide. The fungus not only causes serious yield losses when environmental conditions become favorable (McMullen et al., 1997; Shaner, 2003; Goswami and Kistler, 2004), but also contaminates food and feed products with mycotoxins, such as trichothecenes (e.g., deoxynivalenol) and zearalenones that pose a health risk to humans and animals, thus often leading to significant indirect losses to farmers due to reduced grain quality (Desjardins and Hohn, 1997; Bai and Shaner, 2004; Kazan et al., 2012). On the other hand, like many Fusarium spp, *F. graminearum* is capable of producing several different types of overwinter structures including chlamydospores, thus being recognized as a soil-borne pathogen, and it is known that the fungus also causes seedling crown/root rot on wheat and barley (Roncero et al., 2003; Stephens et al., 2008; Wang et al., 2015, 2018).

The genome of *F. graminearum* (isolate PH-1) consists of four chromosomes (total 36.6 Mb) that have been completely sequenced (Cuomo et al., 2007; King et al., 2015). The most recent assembly released by the Broad Institute (http://www.broadinstitute.org) includes 13,321 proteins (FGSG_00001 through FGSG_13321). A number of FHB-related pathogenicity/virulence factors have been characterized from *F. graminearum* (e.g., Proctor et al., 1995; Lu et al., 2003; Voigt et al., 2005; Jonkers et al., 2012; Zhang et al., 2016; Carere et al., 2017; Lu and Edwards, 2018), but pathogenicity/virulence factors specifically associated with wheat seedling diseases caused by *F. graminearum* have not been reported. Recently, we identified > 30 candidate effector proteins in the *F. graminearum* genome that are transcriptionally induced during FHB development, thus being potentially involved in *F. graminearum*-wheat interactions (Lu and Edwards, 2016). These candidate effector proteins included three (FGSG_00060, 00061 and 00062) with

☆ Mention of trade names or commercial products in this publication is solely for the purpose of providing specific information and does not imply recommendation or endorsement by the U.S. Department of Agriculture. USDA is an equal opportunity provider and employer.

* Corresponding author.
E-mail address: Shunwen.Lu@ars.usda.gov (S. Lu).

https://doi.org/10.1016/j.fgb.2018.11.002
Received 19 September 2018; Received in revised form 8 November 2018; Accepted 8 November 2018
Available online 19 November 2018
1087-1845/ Published by Elsevier Inc.

homology to the KP4 killer toxin protein.

The KP4 protein is one of the three virally encoded proteins (KP1, KP4 and KP6) originally identified from certain strains (P1, P4 and P6, respectively) of the corn smut fungus *Ustilago maydis*. The KP4 protein acts as a killer toxin specifically on certain smut fungi in the order of Ustilaginales (Day and Anagnostakis, 1973; Koltin and Day, 1975), and has no significant sequence similarities with the KP1 and KP6 toxin proteins. The virally encoded KP4 toxin is a 11.3 kD protein with a three-dimensional structure characterized as alpha/beta-sandwich (Ganesa et al., 1989; Gu et al., 1994, 1995; Park et al., 1994) that has been designated as a "Kp4" domain (pfam09044) in the NCBI conserved protein domain database (Marchler-Bauer et al., 2017). The toxicity of the KP4 protein has been associated with the inhibition of cell growth and division by blocking voltage-gated calcium channels and other components in calcium-regulated signal transduction pathways (Gu et al., 1995; Gage et al., 2001; 2002). Transgenic corn (Allen et al., 2011), tobacco (Deb et al., 2018) and wheat (Clausen et al., 2000; Quijano et al., 2016) plants constitutively expressing the KP4 protein have been reported with increased resistance to smut fungi, even certain ascomycetes, i.e., *Alternaria alternata* and *Phoma exigua* var. *exigua* (Deb et al., 2018).

Previous studies (Brown, 2011; Lu and Edwards, 2016) have identified homologues of the KP4 protein from ~20 non-smut fungi and one species of moss. No KP4-like (KP4L) proteins have been functionally characterized to date. We report here the identification and functional analysis of four KP4L proteins from *F. graminearum*. These included the three proteins mentioned above (Lu and Edwards, 2016) and a forth protein (FGSG_10551) identified from additional database searches. We present the genomic structures, full-length mRNA sequences and differential expression patterns of the four *FgKP4L* genes (designated as *FgKP4L-1*, *FgKP4L-2*, *FgKP4L-3* and *FgKP4L-4*, respectively), and describe the heterologous expression and functional analysis of the recombinant FgKP4L proteins and the characterization of *F. graminearum* mutants lacking the *FgKP4L-1*, *-2* and *-3* genes. We also report the identification of KP4L proteins from ~60 additional fungal species and one from amoeba, and we provide evidence that the virally encoded UmKP4 protein and the moss KP4L proteins are closely related to KP4-like proteins identified from a zygomycete and *Aspergillus*, respectively, implying cross-kingdom horizontal gene transfer.

2. Materials and methods

2.1. Fungal isolate and culture conditions

F. gramineraum isolate PH-1 (kindly provided by Dr. Corby Kistler of the USDA-ARS Cereal Disease Laboratory at St. Paul, MN, via Dr. Rubella Goswami) was used in this study. For sporulation, the isolate was recovered from glycerol stocks maintained at −80 °C and grown on agar plates containing potato dextrose (PDA) with quarter strength in a Percival I-36BLL biological incubator (Percival Scientific, Inc, Perry, IA) at 22–24 °C with continuous fluorescent lighting. For liquid cultures, fungal macroconidia were collected from PDA plates and inoculated into 50 ml of complete medium (CM) or minimal medium (MM), which contains glucose as in CM but no nitrogen sources (Leach et al., 1982). The inoculated liquid cultures were incubated at room temperature with slow shaking for two days and left on the bench for an additional 3–14 days before collection of mycelia. Sexual fruiting bodies (perithecia) were obtained on PDA plates following the procedures as described a recent study (Lu and Edwards, 2018). Isolate/strain of the three ascomycetes *Alternaria brassicicola*, *Cochliobolus heterostrophus* and *Nectria haematococca* (used in protein sensitivity tests) were kindly provided by Dr. Gillian Turgeon of Cornell University.

2.2. Nucleic acid preparations

For fungal preparations, mycelia, macroconidia or perithecia were scraped from agar plates or collected from liquid cultures by centrifugation. For plant preparations, spikelets of wheat heads or germinated wheat seeds (healthy or infected by *F. graminearum*) were cut into small pieces with all immature seeds in spikelets (or starch contents in germinated seeds) removed. The collected fungal mycelia or plant tissues were then transferred into 2-ml Lysing Matrix D tubes containing 1.4-mm ceramic spheres (QBiogene, Morgan Irvine, CA) and frozen in liquid nitrogen, followed by homogenization using a Mini-Bead-beater-16 Cell Disrupter (BioSpec Products, Bartlesville, OK). DNA was extracted from the homogenized tissues in cetyl trimethyl ammonium bromide solution (Teknova Inc, Hollister, CA) with chloroform extraction and ethanol precipitation, then finally resuspended in TE buffer (pH 8.0) with the concentration adjusted to 10 to100 ng/μl. mRNA was extracted from the homogenized tissues using the Dynabeads mRNA Direct Kit (Invitrogen, CA) following the manufacturer's instructions and finally eluted in Tris·HCl buffer (pH 8.0). cDNA synthesis was done using the Superscript III first strand synthesis system (Invitrogen, Carlsbad, CA, USA).

2.3. Genomic and cDNA cloning

Genomic clones of the four *FgKP4L* genes, including the entire open reading frames (ORF) and the 5′ and 3′ flanking regions, were obtained by PCR amplification from genomic DNA of PH-1 using primers designed based on the sequences retrieved from the PEDANT genome database (http://mips.helmholtz-muenchen.de/) (Table S1). cDNA clones were obtained by reverse-transcriptase (RT)-PCR using primers designed to the genomic sequence (Table S1). The 5′ and 3′ untranslated regions (UTR) of the *FgKP4L* mRNA transcripts were determined using 5′ and 3′ RACE (rapid amplification of cDNA ends) kits (Invitrogen, Carlsbad, CA), respectively. PCR amplifications were performed using conditions described below. Targeted PCR products were cloned into a pCR2.1 vector using the TOPO TA Cloning Kit with TOP10 chemically competent *E. coli* cells (Invitrogen, Carlsbad, CA). Plasmid DNA was prepared using the Wizard Plus SV Minipreps DNA Purification System (Promega, Madison, WI). Sequence identity was determined by DNA sequencing done at the Cornell University Biotechnology Resource Center using gene- or vector-specific primers. Nucleotide sequences of the genomic and cDNA clones have been deposited into the GenBank database under the accession numbers KY380107 and MH509969 (for genomic DNA) and KY380108 – KY380110, and MG491996 (for mRNA) (Table 1).

2.4. Gene expression profiling

Reverse transcriptase (RT)-PCR was performed to determine the expression patterns of the targeted genes. For tissue-specificity, mRNA samples were isolated from macroconidia, mature perithecia and mycelia (harvested from liquid CM or MM cultures) and protoplasts (from those used for fungal transformation described below), respectively. For temporal expression in axenic cultures, fungal mRNA samples were isolated from mycelia grown in CM or MM liquid cultures at different time points. For temporal expression patterns *in planta*, fungal mRNA samples were isolated (along with the host mRNA) from fungal infected wheat heads that were collected at 4, 12, 24, and 48 h, 4, 8 and 14 d, or the fungal infected seeds at 24, 48, and 72 h, 10 and 13 d post inoculation. DNA oligo primers (Table S1) were designed based on mRNA sequences of individual *FgKP4L* genes and specificity of each set of primers was confirmed by PCR using the plasmid DNA of individual cDNA clones as templates. Concentrations of different cDNA samples were adjusted to be comparable by serial dilutions against the expression level of the *F. graminearum* actin gene (GenBank Acc# XM_011328784), which was used as an internal control. All fungal cDNA samples used for gene expression profiling were first tested to be free of genomic DNA contamination. mRNA samples isolated from uninoculated plants were included as controls to check for possible cross-

Table 1
Main features of KP4-like proteins identified from *F. graminearum*.[a]

Protein	Accession[b]	Size[c]	MW[d]	pI[e]	Domain composition[f]			No of cysteines[g]
					SP	Kp4	CTE	
FgKP4L-1	KY380108	134	12.4	4.5	16	106	12	10 (7.5)
FgKP4L-2	KY380109	125	11.1	4.5	18	99	8	8 (6.4)
FgKP4L-3	KY380110	133	12.1	4.2	16	107	10	10 (7.5)
FgKP4L-4	MG491996	274	27	7.1	18	109/109*	36/1*	12 (4.7)
UmKP4	Q90121	127	11.1	8.6	22	103	2	10 (9.5)

[a] *Ustilago maydis* KP4 protein (UmKP4) is also included in this table for comparison.
[b] Accession indicates the GenBank accession number (www.ncbi.nlm.nih.gov).
[c] Size indicates the number of amino acids in the full-length proteins.
[d] MW, Molecular weight (in kilodaltons), calculated based on the mature proteins.
[e] pI, Isoelectric points, calculated based on the mature proteins.
[f] Numbers in the three columns below indicate the numbers of amino acids consisting of the conserved domains. SP, Signal peptide; Kp4, Kp4 domain (pfam09044); CTE, C-terminal extension after the Kp4 domain (asterisks indicate the numbers for the second Kp4 domain in the FgKP4L-4 protein).
[g] Numbers indicate the cysteine residues in the mature proteins. Numbers in parentheses indicate percentage.

amplification of unrelated wheat genes. All RT-PCR tests were repeated at least twice to verify the observed gene expression patterns.

2.5. PCR conditions

For gene expression profiling, PCR was performed in a 25-µl volume of 1 × GoTaq Green Master Mix (Promega, Madison, WI) that contained 1 µl of cDNA and 0.5 µM each primer. PCR was started with an initial preheat for 5 min at 95 °C, followed by 32–35 cycles of denaturation at 95 °C for 15 s, annealing at 55 or 59 °C for 15 s, and extension at 72 °C for 1–3 min, with a final extension at 72 °C for 10 min. PCR products were separated on a 1% agarose/ethidium bromide gel in TAE buffer. To exclude the possibility of cross-amplification of host genes, the amplified PCR products were purified using the QIAquick PCR Purification Kit (Qiagen, Valencia, CA) and sequenced at the Cornell University Biotechnology Resource Center to confirm the identity of the amplicons. The same PCR conditions were also used for genomic/cDNA cloning of the targeted sequences with size < 3.0 kb. For larger genomic DNA fragments, PCR was done in a 25-µl volume of 1 × LongAmp Taq Master Mix (New England Biolabs, Ipswich, MA) that contained 0.1–0.5 µg of the genomic DNA and 0.5 µM of each primer. PCR began with an initial preheat for 2 min at 94 °C, followed by 32 cycles of denaturation at 94 °C for 20 s, annealing at 52 °C for 30 s, and extension at 65 °C for 5–10 min, with a final extension at 65 °C for 10 min.

2.6. Expression of the recombinant FgKP4L proteins

The coding region corresponding to the mature FgKP4L proteins was PCR-amplified from the corresponding cDNA clone using gene-specific primers with suitable restriction sites incorporated at the 5′ end (Table S1) and sub-cloned into a pPinkα-HC vector (Invitrogen, Carlsbad, CA). The expression construct was transformed into a protease-deficient strain of *Pichia pastoris*, and protein expression and isolation were done as described previously (Lu et al., 2013) following manufacture's procedures which can be downloaded at "https://assets.thermofisher.com/TFS-Assets/LSG/manuals/pichiapink_expression_system_man.pdf". Protein abundance and molecular weight were determined by SDS-PAGE analysis done following standard protocols (Green and Sambrook, 2012). The concentration of the target protein was estimated by comparison with a series of dilutions of bovine serum albumin (BSA) (New England Biolabs, Ipswich, MA) included in the same SDS-PAGE gel. After SDS-PAGE gel separation, the coomassie blue-stained band corresponding to the targeted FgKP4L protein was excised from the gel and subjected to MALDI-TOF/TOF analysis performed at the Cornell University Biotechnology Resource Center as described previously (Lu et al., 2013). Further purification (> 90% purity) of the validated FgKP4L-2 protein was done through a commercial source (GenScript, Piscataway, NJ).

2.7. Targeted gene deletion

The PCR-based split-marker strategy (Turgeon et al., 2010) was used to delete *FgKp4L* genes from the genome. Nucleotide sequences (~1 kb) 5′ upstream or 3′ downstream of the targeted *FgKP4L-1/-2/-3* gene cluster (or the *FgKP4L-4* gene alone) were PCR-amplified from the corresponding genomic DNA clone and then fused with respective sequences of the hygromycin B resistance gene (*hygB*) cassette, which was PCR-amplified from the plasmid pUCATPH (Lu et al., 1994). Primers used to generate desired PCR amplicons are given in Table S1. Transformation of *F. graminearum* (isolate PH-1) was performed using procedures described previously (Lu and Edwards, 2018). Transformants were purified by isolation of single macroconidia from fungal cultures grown on quarter strength PDA plates supplemented with hygromycin B (Sigma-Aldrich, Saint Louis, MO) at 100 µg/ml. The deletion of the targeted gene(s) from the genome was confirmed by PCR screening using gene/locus-specific primers (Table S1).

2.8. Plant materials and bioassays

Hexaploid wheat cultivars BR34 and Grandin are part of our laboratory collections. Additional hexaploid cultivars Auburn (accession number CItr 17898), Bess (PI 642794), Ning 7840 (PI 531188), ND2710 (PI 633976), Russ (PI 592785), Sumai 3 (PI 481542) and Wheaton (PI 469271) were obtained from the National Small Grains Collection of the U.S. National Plant Germplasm System (NPGS). For FHB virulence assays, plants were grown in 6-inch pots (10–16 plants /per pot) containing SB100 professional growing mix (Sungrow Horticulture, Bellevue, WA, USA.) in the greenhouse or a growth chamber at an average temperature of 21 °C with a 16-h photoperiod for 4–5 weeks until anthesis.

For protein activity assays, surface-sterilized wheat seeds were placed on Whatman #1 filter paper in 60 × 15 mm petri dishes (10 seeds/per dish) with 2 ml of the protein solution containing the purified recombinant FgKP4L-2 protein (at a concentration of 30 µg/ml in 0.1 × PBS buffer) added to submerge the seeds. The sample dish was sealed with parafilm and incubated at 30 °C for 24 h, followed by additional incubation at room temperature for 3–5 days. The control seeds were soaked in 0.1 × PBS buffer only or 0.1 × PBS buffer containing the BSA protein ((New England Biolabs) at the same concentration as that of the FgKP4L-2 protein. The shoot and root (radicle only) on germinated seeds were measured individually at 5 days post treatment.

For wheat head (or seed) inoculation, macroconidia were collected from PDA plates and suspended in 0.05% Tween 80 solutions. To determine the FHB-associated temporal expression patterns, wheat heads was inoculated by spreading macroconidial spore suspensions with a sprayer (with the concentration adjusted to 1×10^6/ml). FHB virulence assays of individual deletion mutants were done following the procedures described previously (Lu and Edwards, 2018). For seedling rot-associated expression patterns and virulence assays, surface-sterilized wheat seeds were pre-soaked in 0.5 ml of macroconidial spore suspensions (1×10^5/ml) of the fungus in microcentrifuge tubes with incubation at 30 °C for 24 h. The infected seeds were then planted in soil (SB100 professional growing mix) at the center of 6-inch pots followed by incubation in a growth chamber at an average temperature of 21 °C with a 16-h photoperiod for two weeks. mRNA was isolated from

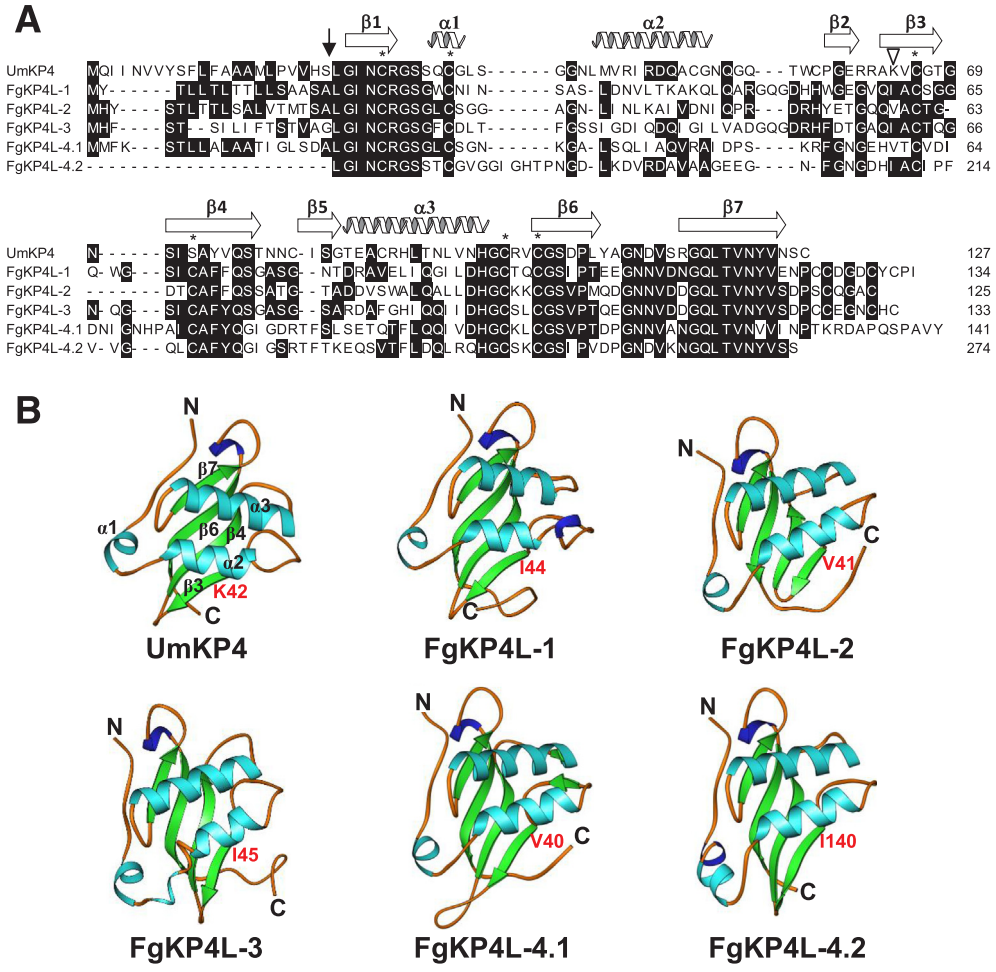

Fig. 1. Sequence alignment and structure prediction of FgKP4-like proteins. (A) Alignment. Identical residues are presented as white letters in a black background. Secondary structures (α, alpha helix; β, beta strand) are drawn based on the *Ustilago maydis* (Um) KP4 protein. Vertical arrow indicates the predicted N-terminal signal peptide cleavage site, which is present in the first (FgKP4L-4.1) but not applicable to the second domain (FgKP4L-4.2) of the FgKp4L-4 protein. Asterisks indicate the positions of conserved cysteine residues. Triangle indicates the position of the lysine residue (K42) in UmKP4 that is essential for activity (Gage et al., 2002). Numbers on the right indicate positions in the full-length protein. (B) Three-dimensional structure prediction. Ribbon diagrams were generated based on the PDB models of the Kp4 domain(s) identified in respective proteins that were predicted by the Protein Homology/Analog Recognition Engine (Kelley et al., 2015). UmKP4 structure was drawn based on PDB accession number 1KPT_A (Gu et al., 1995). Secondary structure elements are highlighted in colors with blue, green and orange for α helices, β strands and loops, respectively. Relative positions of K42 in UmKP4 and the corresponding residues in FgKP4L proteins are indicated near the start point of β3. Note that the three α helices (α1, α2 and α3) and the four larger β strands (β3, β4, β6 and β7) that consists of the β sheet as indicated in the UmKP4 structure are conserved in the Kp4 domain (s) of all FgKP4L proteins. Relative Positions of K42 in UmKP4 and corresponding residues in FgKP4L proteins are indicated (highlighted in red). (For interpretation of the references to colour in this figure legend, the reader is referred to the web version of this article.)

infected seeds/seedling recovered from underground and used for RT-PCR analysis. The number of seedlings emerged from individual pots were recorded 4–14 days after seed planting. The control pot was planted with seeds pre-soaked in water only.

2.9. Sequence, structural and phylogenetic analyses

To identify KP4-like proteins encoded in the genome of *F. graminearum*, the full-length amino acid sequence of the virally-encoded 127-aa *U. maydis* KP4 protein (GenBank accession number Q90121) was used as a query for BLAST searches against the NCBI non-redundant protein sequence database, and the chromosomal locations of the corresponding coding genes were retrieved through the Gene ID browser (www.ncbi.nlm.nih.gov/gene?cmd=Retrieve&dopt) from the annotated *F. graminearum* genome (Cuomo et al., 2007). Amino acid sequence alignments were generated using the MegAlign programs from Lasergene 10.1 software (DNASTAR Inc. Madison, WI). Molecular modeling of the three-dimensional structures of the FgKP4L proteins was done through the PHYRE2 Protein Fold Recognition Server (www.sbg.bio.ic.ac.uk/~phyre2/html) (Kelley et al., 2015). The retrieved PDB files of FgKP4L proteins were examined using the Ribbon program (Carson, 1997). KP4-like proteins from other fungal species were identified through BLASTP searches (Altschul et al., 1997) using the FgKP4L protein sequences as queries against the GenBank databases (www.ncbi.nlm.nih.gov). The N-terminal signal peptides of the fungal KP4-like proteins were determined using the SignalP 4.1 Server (www.cbs.dtu.dk/services/SignalP) and the conserved Kp4 domains were determined using the BLAST CD (conserved domain)-search program (Marchler-Bauer et al., 2017). Phylogenetic analysis was performed using the amino acid sequence alignments of the Kp4 domains generated from the CLUSTALX program (Thompson et al., 1997) and the neighbor-joining method with the PHYLIP 3.696 package (http://evolution.genetics.washington.edu/phylip.html) (Felsenstein, 1989). The PHYLIP-generated unrooted consensus tree (from 1000 bootstrap replicates) was drawn using TreeView software (http://taxonomy.zoology.gla.ac.uk/rod/treeview.html).

3. Results

3.1. Identification of KP4-like proteins encoded in the genome of F. graminearum

Four *F. graminearum* proteins were identified from BLASTP searches and found to have significant similarities [E value = 3×10^{-12} (3e−12) to 2×10^{-15} (2e−15)] to the UmKP4 protein. These were FGSG_00060, 00061 and 00062 reported previously (Lu and Edwards, 2016), and FGSG_10551. These four proteins (all annotated as hypothetical proteins in the databases) were designated in this study as FgKP4L-1, FgKP4L-2, FgKP4L-3 and FgKP4L-4, respectively. The four FgKP4L proteins consisted of 125–274 amino acids (aa) with high percentage (4.7–7.5%) of cysteine residues, and all contained a 16-18-aa N-terminal signal peptide (SP). BLAST Conserved Protein Domain (CD) searches (Marchler-Bauer et al., 2017) confirmed that FgKP4L proteins all contained the Kp4 domain (Pfam09044) with FgKP4L-4 having two Kp4 domains. The predicted mature FgKP4L proteins (11.1–27.0 kDa) were found to be all acidic with isoelectric points

(pI) = 4.2–4.5 except for FgKP4L-4 which appeared to be neutral (pI = 7.1); this was in contrast to the *U. maydis* KP4 protein (UmKP4), which is strongly basic (pI = 8.6) (Table 1).

Amino acid sequence alignment revealed that the Kp4 domains in the four FgKP4L proteins all had conserved residues for secondary structures identified in the UmKP4 protein (Gu et al., 1995). Six conserved cysteine residues were identified with one (the fourth cysteine) missing in UmKP4. The lysine residue in the mature UmKp4 protein (K42) that has been shown to be essential for the killer toxin activity (Gage et al., 2001, 2002) was replaced by a hydrophobic residue isoleucine (I) or valine (V) in all FgKP4L proteins (Fig. 1A). Pair-wise alignments indicated that the Kp4 domains of the FgKP4L proteins all had > 53% similarity to each other (Table S2). The Kp4 domain in the FgKP4L-3 protein had the highest (57%) similarity to the UmKp4 protein (Table S2). Homology-based molecular modeling suggested that all Kp4 domains in the FgKP4L proteins would form a UmKP4-like three-dimensional structure (Gu et al., 1995), which consists of a four-stranded antiparallel β-sheet and two major antiparallel α helices. All three α helices (α1, α 2 and α3) and four larger β strands (β3, β4, β6 and β7) were predicted for UmKP4 and FgKP4L proteins by the same modeling server (Fig. 1B).

3.2. Genomic structure and full-length mRNA transcripts of the FgKP4L genes

All four *FgKP4L* genes were located on the largest chromosome (Chr-1, 11.7 Mb, GenBank accession number NC_026474) with *FgKP4L-1, -2* and *-3* clustered together near the end of the long arm (positions 264309–267672), and *FgKP4L-4* near the end of the short arm (positions 11278548–11279372). These four genes all contained a small (378–825 bp) ORF with the *FgKP4L-1* and *-3* ORFs interrupted by a small intron (52 and 56 bp, respectively), and the *FgKP4L-1* ORF (457 bp) running at a direction opposite to other three genes (Fig. 2A). The identified genomic regions harboring the *FgKP4L-1/-2/-3* cluster (5458 bp) and *FgKP4L-4* (3015 bp) were cloned by PCR amplification from PH-1 genomic DNA. These clones were used for subsequent PCR amplifications of the genomic sequences flanking respective *FgKP4L* genes that are necessary for constructing transforming DNA for the split marker-based gene deletion as described below. The G + C contents of the *FgKP4L* sequences were found to be typical of filamentous ascomycetes (~45%) but within the ORFs, the G + C contents of the introns (37–39%) were much lower than those of the exons (52–54%) (Table S3). These data are consistent with previous observations in that the intronic sequences in eukaryotic genes often have low G + C contents regardless of their size (Lu, 2014; Lu et al., 2017, 2018).

To validate the predicted coding sequences of the *FgKP4L* ORFs, the mRNA transcripts of individual *FgKP4L* genes were obtained by RT-PCR coupled with 5′/3′ RACE cDNA cloning. The assembled full-length *FgKP4L* mRNA transcripts consisted of 620–1368 nucleotides (nt) with an ORF (378–825 nt) that matched the sequences predicted from genomic clones. In addition, the 5′ UTR, the 3′ UTR and the polyA tails were also determined in each *FgKP4L* transcript, and their sizes varied from 58 to 257, 88–251 and 20–46 nt, respectively. The *FgKP4L-4* transcript had the longest 5′ UTR (257 nt) and 3′ UTR (251 nt) (Fig. 2B, Table S4).

3.3. Differential expression of the FgKP4L genes in response to stress conditions

RT-PCR results indicated that the expression levels of the four *FgKP4L* genes in mycelia grown in axenic cultures from liquid minimal medium (MM) or complete medium (CM) were all very low regardless of the duration of incubation time (4 h to 14 d) (Fig. S1). Different cell types, e.g., asexual spores (macroconidia), sexual fruiting bodies (perithecia) and fungal protoplasts were tested. Surprisingly, all four *FgKP4L* genes were found to be expressed (at moderate to high levels) in protoplasts (Fig. 3A, lane 3). Subsequent tests with mycelia grown in "modified" MM medium revealed that this "cell type-related" expression was actually caused by stress conditions associated with protoplast preparations. The expression of the *FgKP4L* genes were all very low in MM medium (Fig. 3B, lane 1), but up-regulated when one or more agents used for protoplast preparation were added into the MM medium, e,g, 0.7 M NaCl, 1.2 M sorbitol, 50 mM $CaCl_2$ and 10 mM Tris base (Fig. 3B, lanes 2–5), or the STC solution which was used to preserve the protoplasts in freezing conditions (Fig. 3B, lane 7). This was especially true for *FgKP4L-3* and *-4*, both of which were up-regulated in response to all these agents (Fig. 3B, bottom two panels). Interestingly, the up-regulation was also observed when 10 mM $ZnSO_4$ was added into the MM medium (Fig. 3B, lane 6). These results suggested that the expression of the *FgKP4L* genes is responsive to stress conditions, like high concentration salts or osmotic pressures rather than different cell types.

3.4. Differential expression of the FgKP4L genes during fungal plant pathogenesis

RT-PCR results indicated that during FHB development, the *FgKP4L-1, -2* and *-3* genes were up-regulated on both susceptible (Wheaton) and resistant (Sumai 3) wheat cultivars with very similar temporal (4 h to 14 d) expression patterns (Fig. S2). In contrast, the *FgKP4L-4* gene appeared to be "silent": no transcripts were detected at any time points on either wheat cultivar (Fig. S2, bottom panel). However, subsequent experiments revealed that all four *FgKP4L* genes were expressed during fungal infection of wheat seedlings.

F. graminearum is known to cause seedling rot in addition to head blight (Wang et al., 2015, 2018), but the infection of wheat seedlings has not been reported for the isolate PH-1. A seedling assay procedure was developed in this study to identify wheat cultivars susceptible to PH-1 infection during seedling development. Eight different hexaploid wheat cultivars (Auburn, Bess, BR34, Grandin, Ning 7840, ND 2710, Russ and Sumai 3) were tested using this seedling assay procedure. Ning 7840 (accession PI 531188) was found to be most susceptible as determined based on the percentage of seedling emergence from PH-1-infected seeds. More than 50% of the Ning 7840 seeds were able to germinate and emerge to the soil surface in the un-inoculated control in contrast to only ~10% from the PH-1-infected seeds of the same cultivar (Fig. 4A). Close examination of the seeds recovered from underground (two weeks post inoculation) revealed that the reduced seedling emergence was due to the fungal infection of the shoot tips at an early stage of the seedling development that resulted in rotted seedlings unable to emerge to the soil surface (Fig. 4B). Ning 7840 was used in subsequent virulence assays for *F. graminearum* mutants generated by targeted gene deletion (see below).

RT-PCR results indicated that all four *FgKP4L* genes were expressed in the fungal-infected seedlings. The clustered *FgKP4L-1, -2* and *-3* genes were all up-regulated in the inoculated seedlings as early as 48 h post inoculation (hpi) and the up-regulated expression was maintained until 10–13 days post inoculation (dpi) (Fig. 4C, panels 2–4, lanes 2–5) at levels much higher than the *in vitro* fungal culture control (lane 6). The *FgKP4L-4* gene was also up-regulated, but appeared to be at certain time points only, e.g., 72 hpi and 13 dpi (Fig. 4C, bottom panel, lanes 3 and 5).

3.5. The recombinant FgKP4L-2 protein possesses root growth-inhibiting activity against wheat

Heterologous expression of recombinant FgKP4L proteins were performed in *Pichia pastoris* and succeeded with the FgKP4L-2 only. The recombinant FgKP4L-2 protein was further purified to ~90% purity from the yeast expressing strain. A single major species with a molecular weight (MW) about 11.1 kD was detected in SDS-PAGE analysis under denaturing conditions (Fig. 5A, lane 1). The purity of the

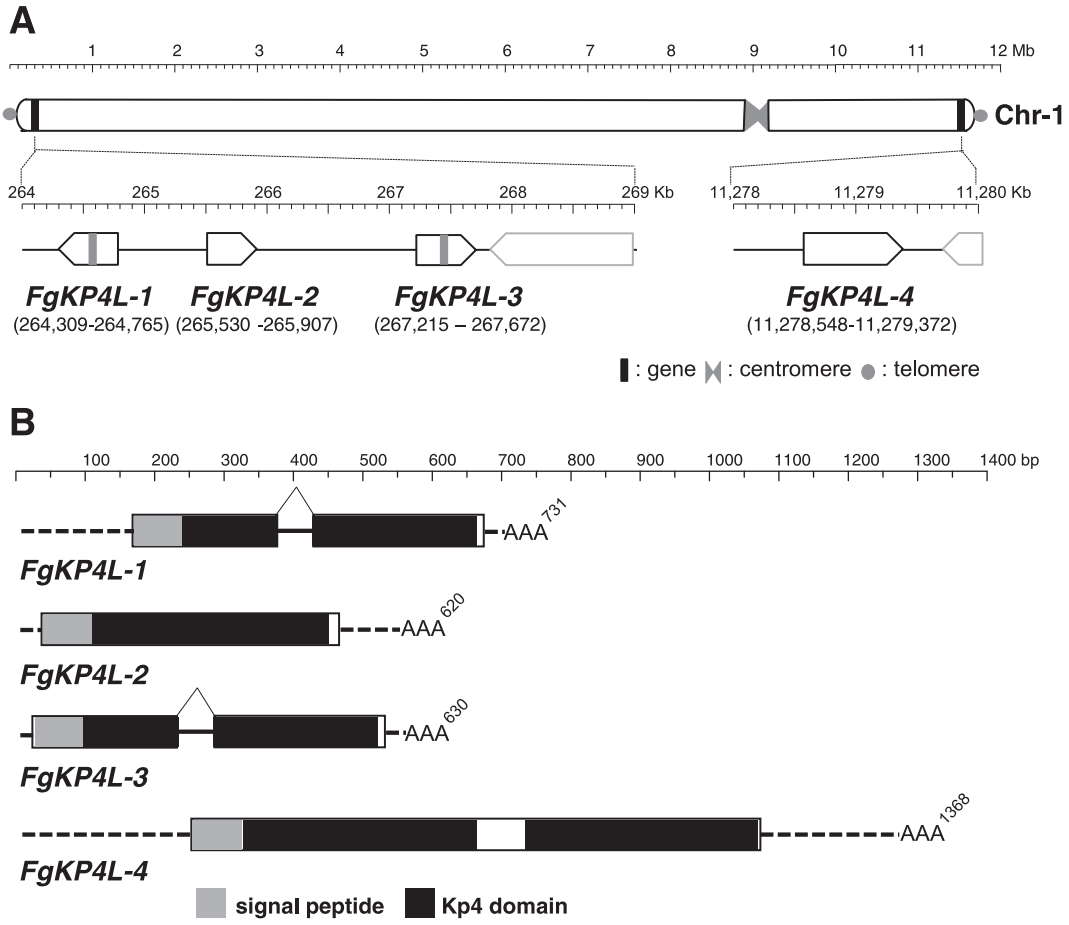

Fig. 2. Genomic organization and full-length mRNA transcripts of the four *FgKP4L* genes identified from *F. graminearum*. (A) Chromosomal locations. The 11.7-Mb Chromosome (Chr) 1 was drawn based on the NCBI Map Viewer (www.ncbi.nlm.nih.gov/genome/?term=fusarium+graminearum). Numbers in parentheses indicate nucleotide positions of the open reading frames of the four *FgKP4L* genes. (B) Structure and domain organization of the full-length mRNA transcripts. Open reading frames are drawn in scale as shown at top (numbers in base pairs). Boxes and thick lines indicate exons and introns (which are spliced in mature mRNA as indicated by brackets). Gray/black fillings indicate exonic regions encoding conserved domains. Dashed lines indicate 5′ and 3′ untranslated regions. AAA: poly-adenosine tail (20–46 bp). Numbers at the end of poly tail indicate the size (bp) of the mature mRNA transcript.

FgKP4L-2 protein appeared to be comparable with the commercially available bovine serum albumin (BSA) protein (Fig. 5A, lane 2). MALDI-TOF/TOF analysis confirmed that the 11.1 kD protein band consisted of only FgKP4L-2-specific peptides.

The recombinant FgKP4L-2 protein did not induce any necrosis when applied to the leaves (by infiltration) or the splikelets (by injection) of FHB-susceptible or resistant wheat lines. However, the same protein was found to be biologically active when tested on wheat seedlings using the seed germination assay procedure, which was developed in this study as prompted by a previous report that the *U. maydis* KP4 protein inhibits plant root growth when tested on Arabidopsis (Allen et al., 2008). The initial test results for the cultivar Ning 7840 are shown in Fig. 5B. At five days post treatment, the length of the shoot and root emerged from the FgKP4L-2 protein-treated seeds (middle panel, left) was apparently shorter than those of the buffer (top panel, left) and the BSA (bottom panel, left) controls. The shoot/root growth of the FgKP4L-2 protein-treated seeds became close to those of the controls when 10 mM $CaCl_2$ was added to the protein solution (compare the three panels on the right). A similar calcium-affected root growth-inhibiting activity was also reported for the *U. maydis* KP4 protein (Allen et al., 2008).

Statistical analysis confirmed that the length average of the root of seedlings treated with the recombinant FgKP4L-2 protein was significantly different from those of the buffer and the BSA controls. At 5 days post treatment, the root length average for the FgKP4L-2-treated seedlings was 1.73 cm, about 48% reduction compared to those of the buffer (3.33 cm) and the BSA (3.37 cm) controls (Fig. 5C). When 10 mM $CaCl_2$ was added to the protein solutions, the root length average of the FgKP4L-2-treated seedlings was increased to 2.33 cm, only slightly different from those of the buffer (2.67 cm) and the BSA (2.77 cm) controls under the same conditions (Fig. 5C). The shoot growth of the FgKP4L-2 treated seedlings was also significantly reduced (data not shown). This reduction was presumably “secondary” due to the poor growth of the root since the shoot itself was not exposure to the protein solutions in test plates.

Interestingly, the inhibition of seedling development by the recombinant FgKP4L-2 protein appeared to be cultivar-dependent. In addition to Ning 7840, Auburn, Bess, BR34 and Sumai 3 also showed sensitivity to the FgKP4L-2 protein treatment with reduced shoot/root growth to different degrees, whereas Grandin, ND495 and Russ did not (Fig. S3). It is still to be determined if the observed root growth-inhibiting activity is wheat-specific. Preliminary experiments indicated that the FgKP4L-2 protein does not affect seedling development of wild tobacco *Nicotiana benthamiana*, or the mycelial growth of three different fungal species, *Alternaria brassicicola*, *Cochliobolus heterostrophus* and *Nectria haematococca* at the same molar concentrations (data not shown).

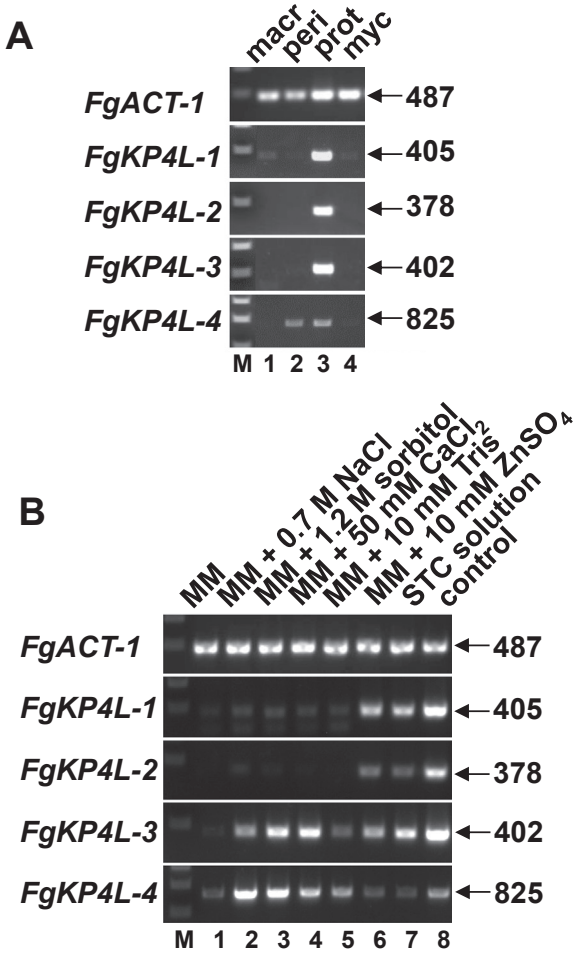

Fig. 3. In vitro expression patterns of the *FgKP4L* genes. Ethidium bromide-stained 1% agarose gels were loaded with the amplicons of RT-PCR products from mRNA isolated from (A), different types of fungal cells, i.e., macroconidia (macr), perithecia (peri), protoplasts (prot) and mycelia (myc, grown in MM, 8 d); (B), fungal mycelia grown in liquid minimal medium (MM) only (lane 1), MM supplemented with individual agents used for protoplast preparation (lanes 2–5), MM supplemented with 10 mM $ZnSO_4$ (lane 6), or in the STC solution used to preserve the protoplasts (lane 7). Control (lane 8) was loaded with RT-PCR products from protoplasts as shown in (A). All mycelial samples were collected at 48 h post inoculation. Numbers at arrow indicate the size of amplicons (in base pairs). *FgACT-1* (*F. graminearum* actin gene) was included as internal controls. M, 1-kb DNA ladder.

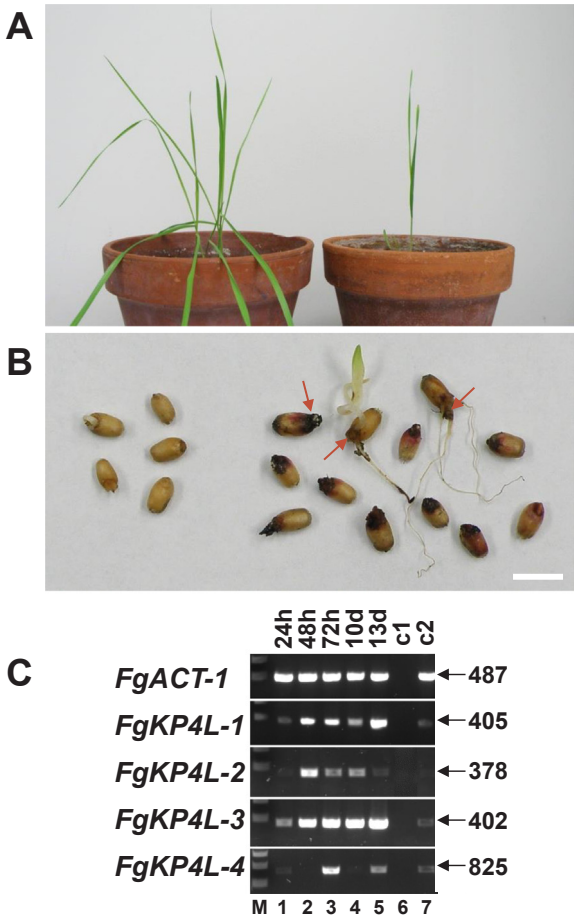

Fig. 4. The four *FgKP4lL* genes are all expressed during fungal infection of wheat seedlings. (A) *F. graminearum* reduces the emergence of wheat seedlings. Potted soils were planted with seeds (15 seeds/per pot) of the hexaploid wheat cultivar Ning 7840 that have been pre-soaked in water (control, left), or in macroconidial suspensions (10^5 spores/per ml) of the isolate PH-1 (right) for 24 h. The emerged seedlings were photographed 13 days post seeding. (B) A photograph showing the diseased seedlings recovered underground from the fungal infected pot shown in (A). Note that most germinated seeds became rotted due to fungal infection of the germinated shoot tips (arrows), in contrast to the five intact un-germinated (or just germinated) seeds on the left that were recovered from the control at the same time. Bars in b = 1 cm. (C) Expression patterns of the four *FgKP4L* genes. Ethidium bromide-stained 1% agarose gels were loaded with the amplicons of RT-PCR products from mRNA isolated from the infected seeds/seedlings of Ning 7840 shown in (A) at 24, 48, 72 h and 10, 13 d post seeding as indicated at the top. Numbers at arrow indicate the size of amplicons (in base pairs). *FgACT-1* (*F. graminearum* actin gene) was included as internal controls. M, 1-kb DNA ladder.

3.6. Deletion of the FgKP4L-1/-2/-3 gene cluster results in reduced virulence in seedling rot on one FgKP4L-2-sensitive wheat cultivar

The clustered *FgKP4L-1, -2* and *-3* genes encode proteins with high similarities (Fig. 1), and they are expressed in similar patterns during FHB development (Fig. S2), suggesting a functional redundancy. To evaluate their roles in fungal pathogenesis more efficiently, the entire genomic region (3425 bp) harboring the *FgKp4L-1/-2/-3* gene cluster was deleted from the genome using the split-marker PCR strategy (Turgeon et al., 2010) (Fig. 6A, left). Fifteen stable hygromycin B-resistant transformants were obtained but only four were found to sustain the targeted deletion as validated by PCR amplification (Fig. 6A, right). The *FgKP4L* ORF-specific primer pairs (1F/1R, 2F/2R and 3F/3R) amplified a 457-bp, 378-bp and 438-bp fragment, respectively, from the wild type control and the transformant TxFg226-3-1 (panels 1–3, lanes 1 and 6), but gave no products from the other four transformants, TxFg226-3-3, 226-3-12, 226-3-14 and 226-3-15 (lanes 2–5). The *hygB*-specific primer pair (pH2150/pH1302) amplified an 849-bp fragment from all five transformants (panel 4, lane 2–6), but gave no products from the wild type control (lane 1). The 5′ end-specific primer pair (5FP and pH2664) amplified a 1144-bp fragment (panel 5) and the 3′ end-specific primer pair (pH431 and 3RP) amplified a 1078-bp fragment (panel 6) from TxFg226-3-3, 226-3-12, 226-3-14 and 226-3-15 (lanes 2–5), but gave no products from TxFg226-3-1 (lane 6). The primer pair 5FP and 3RP (bottom panel) amplified a 5520-bp fragment (harboring the gene cluster) from the wild type control and the TxFg226-3-1 (lanes 1 and 6) but gave a smaller (4632-bp) fragment from the other four transformants (lanes 2–5). These results confirmed that in TxFg226-3-3, 226-3-12, 226-3-14 and 226-3-15, the three native *FgKp4L* genes were completely deleted, while in TxFg226-3-1, the *FgKP4L* gene cluster was intact because the transforming DNA integrated at an “ectopic” location in the genome. All four deletion mutants (Δ*fgkp4l-1-2-3*) and the “ectopic” transformant were found to grow normally and produce

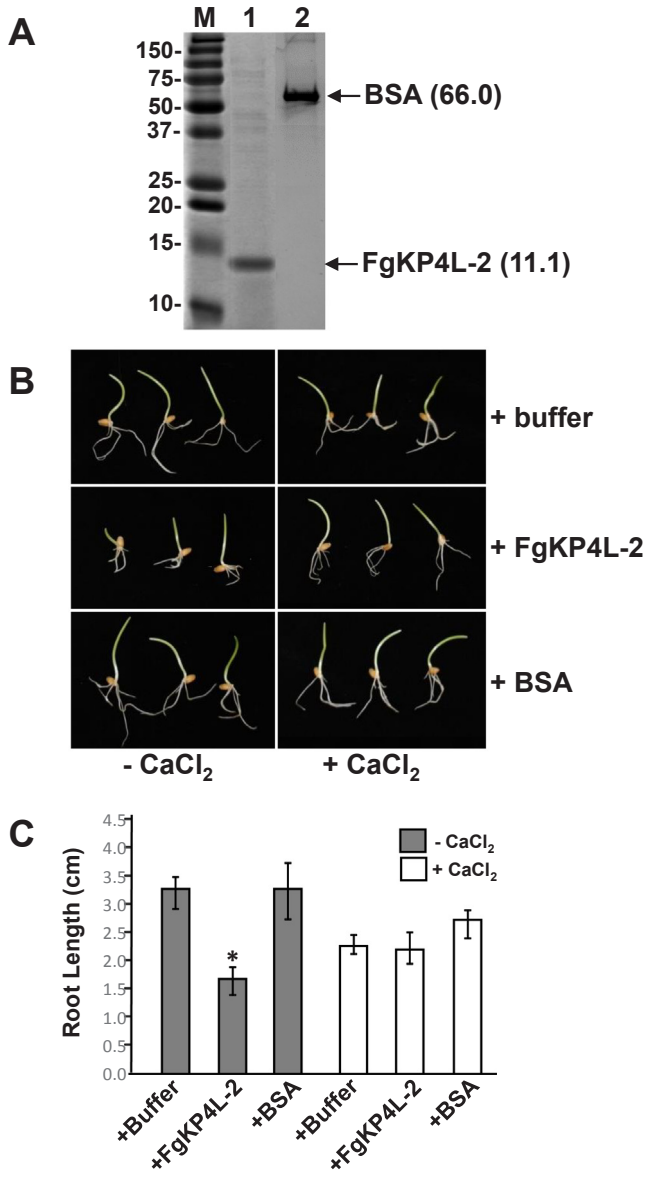

Fig. 5. The recombinant FgKP4L-2 protein possesses biological activity inhibiting root growth of wheat seedlings. (A) Characterization of the recombinant FgKP4L-2 protein. SDS-PAGE gel was loaded (1 μg/per lane) with the purified FgKP4L-2 (lane 1) in comparison with the bovine serum albumin (BSA) protein (lane 2). Numbers on the right indicate the predicted molecular masses (in kD). M, protein markers. The identity of the FgKP4L-2 protein was confirmed by MALDI-TOF/TOF analysis. (B) Seedling assays. Surface-sterilized seeds of the wheat cultivar Ning 7840 were soaked, in the absence (left) or the presence (right) 10 mM $CaCl_2$, in 2 ml of 0.1 × PBS buffer containing the recombinant FgKP4L-2 protein (middle panels) at a concentration of 30 ng/ml. Control seeds were soaked in 0.1 × PBS buffer only (top) or the same concentration of the BSA protein (bottom). Three representative seedlings are shown for each treatment. Photographs were taken five days post treatment. (C) Statistics of the effects of the FgKP4L-2 protein on root growth of wheat seedlings. Columns represent the averages of the root length that was measured on the radicle from a total of 30 seedlings in each treatment as indicated at the bottom. Bars represent standard deviations. Asterisks indicate that the data are significantly different from the controls as determined using a *t*-test ($P < 0.05$).

macroconidia on agar plates like their parental isolate PH-1.

No apparent changes in virulence phenotypes were observed when the Δ*fgkp4l-1-2-3* mutants were tested for FHB on both susceptible (Wheaton) and resistant (Sumai 3) cultivars using the inoculation procedures described previously (Lu and Edwards, 2018). However, subsequent seedling assays revealed that the Δ*fgkp4l-1-2-3* mutants sustained significantly reduced virulence when tested on the PH-1-susceptible and FgKP4L-2-sensitive cultivar, Ning 7840, as determined based on the average percentage of seedling emergence (APSE). At 14 days post seed planting (dpp), only one or two seedlings emerged from the pot with seeds infected by the wild type isolate PH-1 (Fig. 6B, pot #1) or the ectopic transformant TxFg226-3-1 (pot #6), whereas more seedlings emerged from the pots inoculated with any of the four Δ*fgkp4l-1-2-3* mutants (pot #2–5). that were more or less comparable to the un-inoculated control. The calculated APSE (based on three independent tests) was 53% for the un-inoculated control, 13% and 11% for those inoculated with the wild type isolate and the ectopic transformant, respectively, and 29–33% for those inoculated with individual Δ*fgkp4l-1-2-3* mutants (Fig. 6C). A *t*-test confirmed that the differences between the wild type and the four deletion mutants were all significant ($P < 0.05$), whereas no significant differences were observed between the wild type and the ectopic transformant (Fig. 6C). These data indicated that the deletion of the *FgKP4L-1-2-3* gene cluster results in a ~20% reduction in fungal virulence in seedling rot on this particular wheat cultivar. Further complementation test was found not feasible because no sufficient amount of protoplasts can be isolated from the Δ*fgkp4l-1-2-3* mutants, presumably due to the possible involvement of the *FgKP4L* genes in stabilization of the protoplasts since they were all up-regulated in protoplasts as observed in the expression profiling experiments (Fig. 3). It is still to be determined if this problem can be resolved through optimization of the culture and/or the enzyme-osmoticum conditions in protoplast preparation.

3.7. KP4-like proteins are found in diverse fungi and also in moss and amoeba

BLAST searches identified > 200 fungal KP4-like (KP4L) proteins from a total of 85 species belonging to Ascomycota (79), Basidiomycota (5) or Zoopagomycota (1). Most ascomycetes came from two classes, i.e., Sordariomycetes (46) and Eurotiomycetes (20) with most Sordariomycete species coming from three genera, i.e., *Fusarium* (12), *Metarhizium* (8) and *Trichoderma* (11) (Table 2). Twenty-nine double domain KP4L proteins were identified, and all (except for two) were found in Sordariomycetes (Table 2). About half of the fungal species were human-animal pathogens, including those common species, e.g., *Blastomyces dermatitidis* and *Histoplasma capsulatum* and opportunistic pathogens, e.g., *Aspergillus oryzae* and *Fusarium solani*. Most fungal species were found to have multiple (2–6) KP4L proteins with *Basidiobolus meristosporus* (a zygomycete) having the highest number (8) of KP4L proteins (Table S5). Only two non-fungal species were found to have KP4L proteins, including the moss *Physcomitrella patens* (Php) reported previously (Brown, 2011) and *Planoprotostelium fungivorum* (a species of amoeba) (Pf) identified in this study, both of which have two single domain KP4L proteins (GenBank accession numbers XP_001777496 and XP_001777519 for Php, and PRP75338 and PRP75353 for Pf, respectively).

An amino acid sequence alignment indicated that the Kp4 domain (s) of the identified KP4L proteins contained six highly conserved cysteine (C1–C6) residues. C1, C2, C5 and C6 were strictly conserved in all aligned proteins. C3 was missing in the zygromycete *Basidiobolus meristosporus* (Bam). C4 was missing in the virally encoded *U. maydis* KP4 (UmKP4) protein, BamKP4Ls and KP4L proteins identified from the ascomycetes *Clohesyomyces aquatic* (Ca) and *Coniosporium apollinis* (Coa) (Fig. S4). Noticeably, the active site K42 in the UmKP4 protein (Gage et al., 2002) was replaced by a hydrophobic residue, predominantly, isoleucine (I), leucine (L) and valine (V), in all aligned KP4L proteins including those identified from the two non-fungal species (Fig. S4).

Phylogenetic analysis revealed that a majority of fungal KP4L proteins fall into four major groups (Fig. 7). Group I consisted of all Sordariomycetes except for one (*Pseudogymnoascus sp*) from Leotiomycetes.

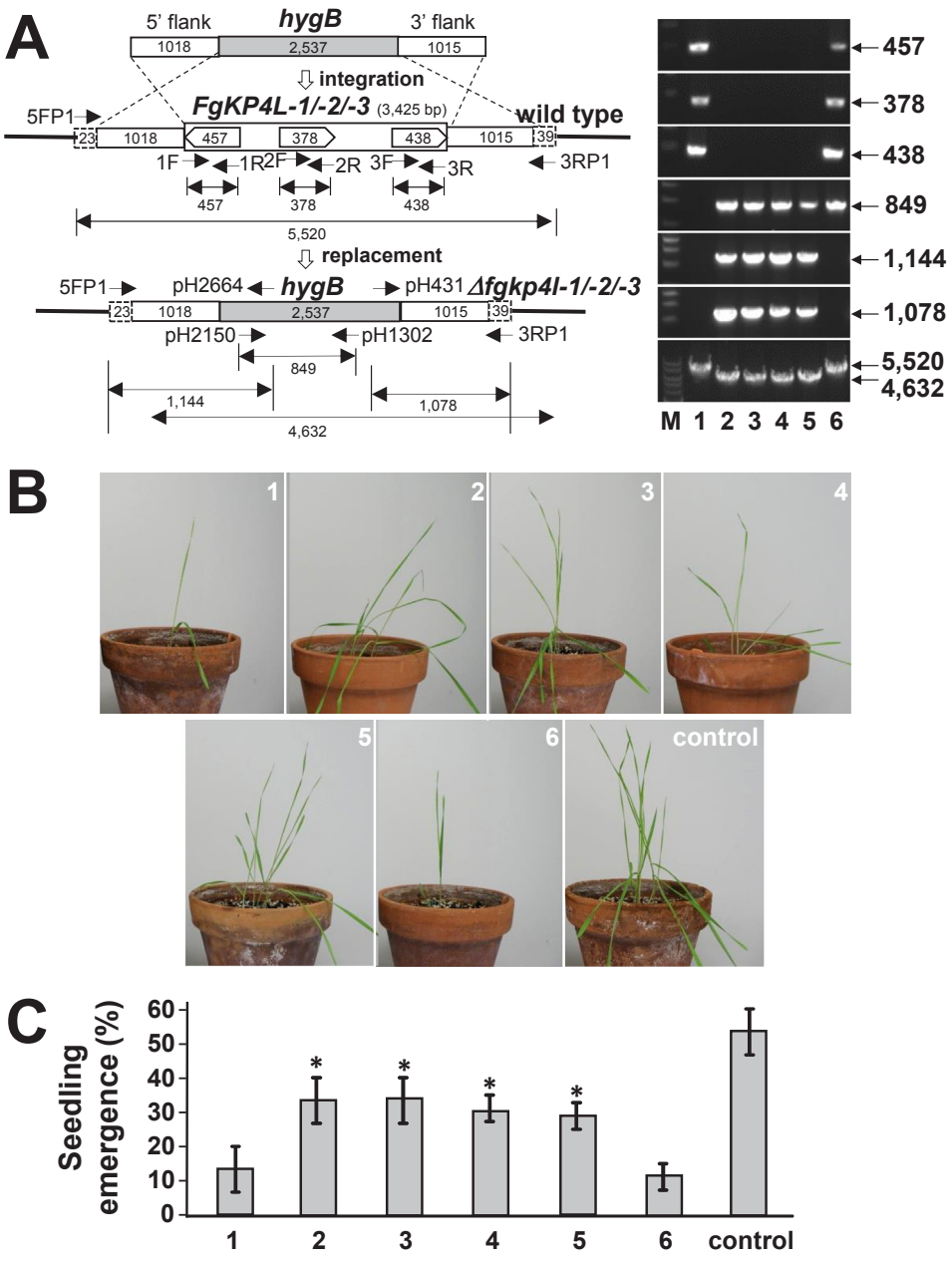

Fig. 6. Deletion of the *FgKP4L-1/-2/-3* gene cluster results in reduced virulence in seedling rot on FgKP4L-2-sensitive wheat. (A) Characterization of the deletion mutants. Left: Schematic representation of the split marker strategy used to knockout the gene cluster. Open boxes, filled boxes, open arrows, and open boxes with dashed lines represent PCR fragments (or the corresponding genomic sequences), the hygromycin B (*hygB*) resistance gene cassette, the *FgKP4L* gene open reading frame, and the genomic sequences 5′ or 3′ outside of the targeted genomic regions, respectively; numbers inside indicate the size (in base pairs). Thick lines indicate *F. graminearum* genome sequence. Dashed cross lines indicate the expected crossover between homologous sequences. Arrows indicate the primers (Table S1) used to validate the integration events and the expected PCR products with size are indicated by double-arrowed lines. Right: PCR-validation of the targeted deletion events. Ethidium bromide-stained gels were loaded with PCR products amplified from DNA of the wild type parental isolate PH-1 (lane 1) and five transformants, TxFg226-3-3, 226-3-12, 226-3-14, 226-3-15, and 226-3-1 (lanes 2–6). Numbers on the right indicate size (in base pairs) of the expected amplicons shown in (A). M, 1-kb DNA ladder. (B) Seedling assays showing the virulence phenotypes of the wild type isolate PH-1 (pot 1) and the five transformants (pots 2–6) in the same order as in the gels shown in (A). Wheat seeds of the FgKP4L-2-sensitive cultivar Ning 7840 were pre-soaked with macroconidial suspensions of the fungus *in vitro* for 24 h and then planted in soils (15 seeds/pot) to allow to germinate naturally. One representative pot was shown for each treatment. Photographs were taken 13 days post planting. (C) Statistics of the seedling emergence from the seven treatments shown in (B). Columns represent the averages of the percentage of seedling emergence that were calculated from three independent tests. Bars represent standard deviations. Asterisks indicate a significant difference from that of the wild type isolate (determined by a *t*-test at $P < 0.05$).

The FgKP4L-1, -2 and -3 proteins were all found in this group, each represented a sub-clade. Group II included exclusively all KP4Lproteins that contain double Kp4 domains (designated as “a” and “b” for convenience) as represented by the FgKP4L-4 protein. All these double domain KPL proteins came from Sordariomycetes except for *Pseudogymnoascus sp*. Group III, which consisted of species from three classes, i.e., Sordariomycetes, Lecanomycetes and Leotiomycetes. Group IV included mainly Eurotiomycetes (most from *Apergillus*), but also the two from the moss *Physcomitrella patens* (Fig. 7). In addition, two minor groups (Group v and vi) were also recognizable. Group v consisted of several Sordariomycetes (all from *Trichoderma*) and three human-pathogenic Eurotiomycetes. Group vi (the smallest group) consisted of all KP4L proteins from the zygomycete *Basidiobolus meristosporus* and the virally-encoded UmKP4 protein. The six groups in the phylogenetic tree were all supported (> 55% confidence) by bootstrapping analysis (Fig. 7).

4. Discussion

The virally encoded KP4 killer toxin protein was first identified from the corn smut fungus *U. maydis* as early as the 1970s (Day and Anagnostakis, 1973; Koltin and Day, 1975), and homologues were later identified from the genomes of ~20 fungal species (Brown, 2011; Lu and Edwards, 2016). Until now, the function of these fungal KP4-like (KP4L) proteins has not been characterized to any degree in ascomycetes. In this study, we identified and characterized four KP4L proteins in *F. graminearum* and provided evidence that FgKP4L proteins are biologically active with commonalities with the virally encoded UmKP4 protein, and the *FgKP4L* genes may function in virulence during fungal plant pathogenesis.

4.1. Characteristics of the FgKP4L proteins and differential expression of the coding genes

The four FgKP4L proteins share striking sequence and structure similarities with the UmKP4 protein. However, the FgKP4L proteins all

Table 2
KP4-like proteins identified in the kingdom Fungi.

Division/Class[a]	#Sp[b]	#Pro[c]	#2Kp4[d]	Genera[e]
Ascomycota	**79**	**195**	**29**	
Dothideomycetes	7	8	0	*Alternaria*, *Clohesyomyces*, *Coniosporium*, *Glonium stellatum*, *Parastagonospora*, *Paraphaeosphaeria*, *Stagonospora*
Eurotiomycetes	20	28	0	*Aspergillus* (9), *Blastomyces* (3), *Emergomyces*, *Emmonsia* (2), *Helicocarpus*, *Histoplasma*, *Penicillium* (2) *Penicilliopsis*
Lecanoromycetes	1	4	0	*Umbilicaria*
Leotiomycetes	2	8	2	*Pseudogymnoascus*
Orbiliomycetes	2	2	0	*Arthrobotrys*, *Dactylellina*
Sordariomycetes	46	144	27	*Cordyceps* (3), *Eutypa*, *Fusarium* (13), *Grosmannia*, *Hirsutella*, *Hypoxylon* (3), *Isaria*, *Metarhizium* (8), *Ophiocordyceps*, *Ophiostoma*, *Pochonia*, *Purpureocillium*, *Tolypocladium*, *Trichoderma* (10)
Xylonomycetes	1	1	0	*Xylona*
Basidiomycota	**5**	**8**	**0**	
Agaricomycetes	4	7	0	*Auricularia*, *Exidia*, *Moniliophthora*
Ustilaginomycetes	1	1	0	*Ustilago*
Zoopagomycota	**1**	**8**	**0**	
Basidiobolomycetes 1	1	8	*0*	*Basidiobolus*
Total	**85**	**211**	**29**	

[a] Fungal classification follows the NCBI taxonomy system (www.ncbi.nlm.nih.gov/taxonomy/?term = fungi). Classes with more than five KP4-like protein-containing species are underlined.

[b] Numbers indicate the identified species containing KP4-like protein (s). A complete list of the related genera/species is given in Table S5.

[c] Numbers indicate the KP4-like proteins identified through BLASTP searches against the NCBI non-redundant protein database with the *Ustilago maydis* KP4 protein (GenBank accession number Q90121) as a query and a cut-off E value $< 1e-5$. Homologues from different isolates (strains) of the same species were counted only once from a representative with whole genome sequence available or well known in the research area.

[d] Numbers indicate the KP4-like proteins that contain double Kp4 domain (pfam09044) as determined by BLAST conserved domain (CD) search (www.ncbi.nlm.nih.gov/Structure/cdd/wrpsb.cgi?).

[e] Numbers in parentheses indicate the number of the species (if more than one) within the genus that contains KP4-like protein(s). Genera with more than five KP4-like protein-containing species are underlined.

have six conserved cysteine residues whereas the UmKP4 protein has only five. In addition, the lysine residue (K42) in the UmKP4 protein that has been shown to be essential for the killer toxin activity (Gage et al., 2002) is replaced by a hydrophobic residue, i.e., isoleucine (I) or valine (V) in all FgKP4L proteins (Fig. 1). Further analysis confirmed that the conservation of the six cysteine residues in predominant, and the hydrophobic residue replacement is strictly conserved among all KP4L proteins included in the sequence analysis (Fig. S4). It will be interesting to investigate if these variations are associated with the different root growth-inhibiting activities observed for the FgKP4L-2 protein on wheat and the UmKP4 protein on Arabidopsis (Allen et al., 2008).

All *FgKP4L* genes are located on chromosome 1 (Fig. 2A) with high sequence similarities with each other (Table 3, Table S2), suggesting that they have a common ancestor. However, *FgKP4L-1* and *-3* genes contain one intron in the ORF, whereas *FgKP4L-2* and *-4* lack any introns in the ORF. *FgKP4L-4* encodes double Kp4 domains, whereas other three genes encode only one (Fig. 2B, Table S4). These genomic variations may reflect substantial sequence diversifications associated with fungal genome evolution.

Transcriptional analysis revealed that all *FgKP4L* genes are expressed at very low levels in fungal mycelia grown in axenic cultures, especially in minimal medium (Fig. S1), but all are up-regulated under certain stress conditions (Fig. 3) and in fungal plant pathogenesis (Fig. 3B), suggesting that they may be under the control of certain common regulatory pathways. However, the *FgKP4L-3* and *-4* genes appear to be more sensitive to stress signals, and the *FgKP4L-4* gene is expressed in seedling rot but not in FHB development (Fig. 4C, Fig. S2). It will be interesting to investigate if these non-common expression patterns are due to the variations found in the 5′ untranslated region of individual *FgKP4L* mRNA sequences (Fig. 2, Table S4).

4.2. Biological activity of the recombinant FgKP4L-2 protein

Previous studies have been shown that the virally encoded UmKP4 protein acts as a killer toxin by blocking calcium channels in fungal and mammalian cells (Gu et al., 1995; Gage et al., 2001, 2002), and the same toxin protein also inhibits plant root growth in a calcium-affected manner when tested *in vitro* on a dicotyledonous plant, *Arabidopsis thaliana* (Allen et al., 2008). In this study, we demonstrated that the FgKP4L-2 protein also inhibits plant root growth *in vitro*, but on a monocotyledonous plant species, common wheat (Fig. 5). It will be interesting to test if FgKP4L-2 also inhibits root growth on *A. thaliana*, although our preliminary tests indicated that it does not do so on the dicotyledonous *N. benthamiana*. It is likely that different KP4L proteins have different host specificities. On the other hand, the inhibition of Arabidopsis root growth by UmKP4 (Gage et al., 2002) and inhibition of wheat root growth by FgKP4L-2 (this study) are observed at comparable micromolar concentrations (i.e., 3–8 μM), and the root growth-inhibiting activities of both UmKP4 and FgKP4L-2 proteins are partially abrogated by exogenously added calcium. These commonalities suggest that like UmKP4, FgKP4L proteins may also act as blockers of calcium channel proteins commonly found in cell membranes of eukaryotic cells.

Interestingly, the activity of the FgKP4L-2 protein appears be cultivar-dependent because the inhibition of root growth was observed only on certain wheat cultivars under the conditions used in this study (Fig. S3). This observation opened the door for further studies to determine if the FgKP4L-2 protein may act as a host-selective toxin (HST) as those proteinaceous HSTs characterized in previous studies (reviewed by Ciuffetti et al., 2010; Oliver et al., 2012).

4.3. The function of the FgKP4L genes in fungal plant pathogenesis

The expression of the *FgKP4-1*, *-2* and *-3* genes are all tightly associated with fungal pathogenesis in both FHB (Fig. S2) and seedling rot (Fig. 4) on wheat. However, the deletion of the *FgKP4-1/-2/-3* gene cluster results in reduced virulence in seedling rot (Fig. 6) but not in FHB. It is known that calcium is present in soils as a divalent ion (Ca^{2+}), taken up by plants through root cells that are rich in Ca^{2+}-permeable channels on plasma membranes, and subsequently translocated to all aboveground tissues of the plants (White and Broadley, 2003; Gilliham et al., 2011). TaTPC1, the calcium channel protein identified from wheat has been shown to be expressed exclusively in roots (Wang et al., 2005). Thus, the deletion of the *FgKP4-1-2-3* gene cluster does not affect fungal virulence in FHB because the wheat cells

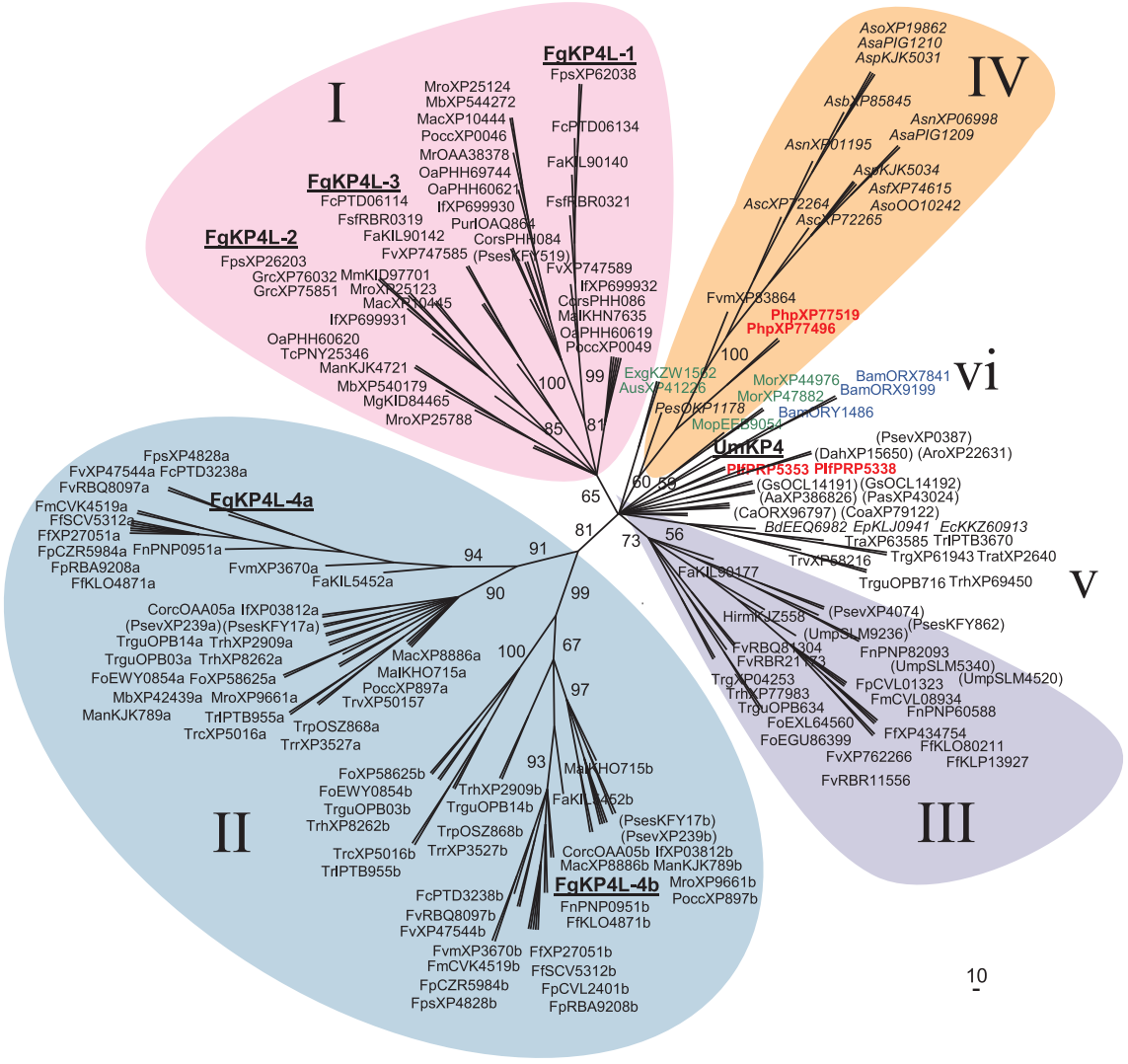

Fig. 7. Phylogenetic relationship of KP4-like proteins. The neighbor-joining tree was generated based on the conserved Kp4 domain sequences. Bootstrapping values (> 50%, from 1000 replicates) are indicated on major branches. Protein names are given as species abbreviations followed by Genbank accession numbers (beginning letters plus the last 4–5 numbers only): Php, *Physcomitrella patens* (moss); Plf, *Planoprotostelium fungivorum* (amoeba). Abbreviations for all fungal species in the tree are given in Table S5. Proteins with double Kp4 domains are distinguished by the letter "a" and "b" at the end of the protein names. The four FgKP4L and the *Ustilago maydis* KP4 (UmKP4) proteins are underlined. Proteins from Ascomycota, Basidiomycota, Zoopagomycota and non-fungal organisms (Php and Plf) are highlighted in black, green, blue and red, respectively. Proteins from Eurotiomycetes are in italics and all other ascomycete classes are in parentheses. The four major groups (Group I–IV) are shaded in colors. Note that FgKP4L-1, -2, and -3, each represents a "sister" clade in Group I, whereas FgKP4L-4 is located Group II, which includes all proteins with double Kp4 domains. Note also that UmKP4 is located in a minor group (Group v) with the KP4L proteins from the zygomycete *Basidiobolus meristosporus* (Bam), and the two moss KP4L proteins (Php) are located in Group IV together with Eurotiomycetes.

comprising the spikelets may lack the targeted calcium channel proteins. The up-regulation of the *FgKP4L* genes during FHB development may be associated with certain host-derived "stress" signals. Additional experiments are needed to obtain Δ*fgkp4l-4* mutants to address if the *FgKP4L-4* gene also contributes to seedling rot disease although it is expressed only at certain time points during seedling rot infection (Fig. 4C).

It should be noted that four FgKP4L-2-sensitive wheat cultivars (Auburn, Bess, BR34 and Sumai 3) are notsusceptible to the fungus in seedling infection assays as Ning 7840 when tested under the same conditions (data not shown). This observation suggests that although involved in virulence, the FgKP4L proteins may only play minor roles in seedling rot disease, thus the impact of the native FgKP4L-2 protein on seedling development may be compensated by resistance pathways in certain wheat cultivars such as the four tested in the FgKP4L-2 sensitivity assays (Fig. S3).

4.4. The distribution of the KP4L proteins among fungi and other eukaryotic organisms

A previous study (Brown, 2011) has explored the distribution and the relationships between KP4-like proteins, but the analysis was based on 18 fungal species only (17 ascomycetes, one basidiomycete and with no zygomycetes). The data obtained in this study (from 85 diverse fungal species including one zygomycete) allowed us to infer phylogenetic relationships of different groups of KP4-like proteins with a much better resolution. It is clear that the FgKP4L proteins represent only two of the four major groups, i.e., FgKP4L-1, -2 and -3 for Group I, and FgKP4L-4 for Group II (Fig. 7), suggesting that the KP4L proteins in other groups may have distinct function(s) depending on the species. The fact that more than half of the KP4L proteins come from human-animal pathogens (Table S5) emphasizes the medical importance of studies on this group of proteins. It is noticeable that the KP4L proteins identified from Dothideomycetes (Ascomycota) or agaricomyceys

(Basidiomycota) do not form a separate group by themselves or group together with other species (Fig. 7), implying extensive sequence divergence or frequent losses of the coding genes in these two groups of fungi.

There are two particular interesting points in the phylogenetic tree (Fig. 7). First, the two KP4L proteins identified from the moss *Physcomitrella patens* are found in the same group (Group IV) with *Aspergillus* spp (60% confidence), suggesting strongly that a cross-kingdom horizontal gene transfer (HGT) may have occurred between plant and fungi. It is also possible that the two KP4L proteins identified from the amoeba *Planoprotostelium fungivorum* is associated with HGT although this possibility is not resolved in the same phylogenetic tree. Second, the UmKP4 protein is found in the same minor group (Group vi) with the zygomycete *Basidiobolus meristosporus*. This replacement is also well supported by bootstrapping analysis (> 60% confidence), thus raising the possibility that the *U. maydis*-hosted virus may have acquired the *KP4* gene from an extinct species of zygromycetes.

In summary, through database-mining and heterologous expression, we have identified four KP4-like (KP4L) proteins from *F. graminearum*, an economically important pathogen of cereal crops and characterized the first recombinant fungal KP4L protein. The seedling assay methods developed in this study and targeted gene deletion analysis provided evidence that FgKP4L proteins possess root growth inhibiting activity against wheat and potentially contribute to fungal virulence in seedling rot on wheat. Further studies on FgKP4L proteins would help elucidate the roles of the fungal KP4L proteins in diverse host-pathogen interactions.

Acknowledgements

We thank Cayley Steen for technical assistance. This study was supported by United States Department of Agriculture, Agricultural Research Service CRIS project 3060-21000-038-00D.

Appendix A. Supplementary material

Supplementary data to this article can be found online at https://doi.org/10.1016/j.fgb.2018.11.002.

References

Allen, A., Islamovic, E., Kaur, J., Gold, S., Shah, D., Smith, T.J., 2011. Transgenic maize plants expressing the Totivirus antifungal protein, KP4, are highly resistant to corn smut. Plant Biotechnol. J. 9, 857–864.
Allen, A., Snyder, A.K., Preuss, M., Nielsen, E.E., Shah, D.M., Smith, T.J., 2008. Plant defensins and virally encoded fungal toxin KP4 inhibit plant root growth. Planta 227, 331–339.
Altschul, S.F., Madden, T.L., Schaffer, A.A., Zhang, J., Zhang, Z., Miller, W., Lipman, D.J., 1997. Gapped BLAST and PSI-BLAST: a new generation of protein database search programs. Nucleic Acids Res. 25, 3389–3402.
Bai, G., Shaner, G., 2004. Management and resistance in wheat and barley to Fusarium head blight. Ann. Rev. Phytopathol. 42, 135–161.
Brown, D.W., 2011. The KP4 killer protein gene family. Curr. Genet. 57, 51–62.
Carere, J., Benfield, A.H., Ollivier, M., Liu, C.J., Kazan, K., Gardiner, D.M., 2017. A tomatinase-like enzyme acts as a virulence factor in the wheat pathogen *Fusarium graminearum*. Fungal Genet. Biol. 100, 33–41.
Carson, M., 1997. Ribbons. Methods Enzymol. 277, 493–505.
Ciuffetti, L.M., Manning, V.A., Pandelova, I., Betts, M.F., Martinez, J.P., 2010. Host-selective toxins, Ptr ToxA and Ptr ToxB, as necrotrophic effectors in the *Pyrenophora tritici-repentis*-wheat interaction. New Phytol. 187, 911–919.
Clausen, M., Krauter, R., Schachermayr, G., Potrykus, I., Sautter, C., 2000. Antifungal activity of a virally encoded gene in transgenic wheat. Nat. Biotechnol. 18, 446–469.
Cuomo, C.A., Guldener, U., Xu, J.R., Trail, F., Turgeon, B.G., Di Pietro, A., Walton, J.D., Ma, L.J., Baker, S.E., Rep, M., Adam, G., Antoniw, J., Baldwin, T., Calvo, S., Chang, Y.L., Decaprio, D., Gale, L.R., Gnerre, S., Goswami, R.S., Hammond-Kosack, K., Harris, L.J., Hilburn, K., Kennell, J.C., Kroken, S., Magnuson, J.K., Mannhaupt, G., Mauceli, E., Mewes, H.W., Mitterbauer, R., Muehlbauer, G., Munsterkotter, M., Nelson, D., O'Donnell, K., Ouellet, T., Qi, W., Quesneville, H., Roncero, M.I., Seong, K.Y., Tetko, I.V., Urban, M., Waalwijk, C., Ward, T.J., Yao, J., Birren, B.W., Kistler, H.C., 2007. The *Fusarium graminearum* genome reveals a link between localized polymorphism and pathogen specialization. Science 317, 1400–1402.
Day, P., Anagnostakis, S., 1973. The killer system in *Ustilago maydis*: heterokaryon transfer and loss of determinants. Phytopathology 63, 1017–1018.
Deb, D., Shrestha, A., Maiti, I.B., Dey, N., 2018. Recombinant promoter (MUASCsV8CP) driven totiviral killer protein 4 (KP4) imparts resistance against fungal pathogens in transgenic tobacco. Front. Plant Sci. 9, 278.
Desjardins, A.E., Hohn, T.M., 1997. Mycotoxins in plant pathogenesis. Mol. Plant-Microbe Interact. 10, 147–152.
Felsenstein, J., 1989. Mathematics vs. evolution: mathematical evolutionary theory. Science 246, 941–942.
Gage, M.J., Bruenn, J., Fischer, M., Sanders, D., Smith, T.J., 2001. KP4 fungal toxin inhibits growth in *Ustilago maydis* by blocking calcium uptake. Mol. Microbiol. 41, 775–785.
Gage, M.J., Rane, S.G., Hockerman, G.H., Smith, T.J., 2002. The virally encoded fungal toxin KP4 specifically blocks L-type voltage-gated calcium channels. Mol. Pharmacol. 61, 936–944.
Ganesa, C., Chang, Y.J., Flurkey, W.H., Randhawa, Z.I., Bozarth, R.F., 1989. Purification and molecular properties of the toxin coded by *Ustilago maydis* virus P4. Biochem. Biophys. Res. Commun. 162, 651–657.
Gilliham, M., Dayod, M., Hocking, B.J., Xu, B., Conn, S.J., Kaiser, B.N., Leigh, R.A., Tyerman, S.D., 2011. Calcium delivery and storage in plant leaves: exploring the link with water flow. J. Exp. Bot. 62, 2233–2350.
Goswami, R.S., Kistler, H.C., 2004. Heading for disaster: *Fusarium graminearum* on cereal crops. Mol. Plant Pathol. 5, 515–525.
Green, M. R., Sambrook, J., 2012. Molecular Cloning: A Laboratory Manual (Fourth Edition). Cold Spring Harbor Laboratory Press, Cold Spring Harbor, NY, pp 1890.
Gu, F., Khimani, A., Rane, S.G., Flurkey, W.H., Bozarth, R.F., Smith, T.J., 1995. Structure and function of a virally encoded fungal toxin from *Ustilago maydis*: a fungal and mammalian Ca^{2+} channel inhibitor. Structure 3, 805–814.
Gu, F., Sullivan, T.S., Che, Z., Ganesa, C., Flurkey, W.H., Bozarth, R.F., Smith, T.J., 1994. The characterization and crystallization of a virally encoded *Ustilago maydis* KP4 toxin. J. Mol. Biol. 243, 792–795.
Jonkers, W., Dong, Y., Broz, K., Kistler, H.C., 2012. The Wor1-like protein Fgp1 regulates pathogenicity, toxin synthesis and reproduction in the phytopathogenic fungus *Fusarium graminearum*. PLoS Pathog. 8, e1002724.
Kazan, K., Gardiner, D.M., Manners, J.M., 2012. On the trail of a cereal killer: recent advances in *Fusarium graminearum* pathogenomics and host resistance. Mol. Plant Pathol. 13, 399–413.
Kelley, L.A., Mezulis, S., Yates, C.M., Wass, M.N., Sternberg, M.J., 2015. The Phyre2 web portal for protein modeling, prediction and analysis. Nat. Protoc. 10, 845–858.
King, R., Urban, M., Hammond-Kosack, M.C., Hassani-Pak, K., Hammond-Kosack, K.E., 2015. The completed genome sequence of the pathogenic ascomycete fungus *Fusarium graminearum*. BMC Genomics 16, 544.
Koltin, Y., Day, P.R., 1975. Specificity of *Ustilago maydis* killer proteins. Appl. Microbiol. 30, 694–696.
Leach, J., Lang, B.R., Yoder, O.C., 1982. Methods for selection of mutants and in vitro culture of *Cochliobolus heterostrophus*. Microbiology 128, 1719–1729.
Lu, S., 2014. Zn^{2+} blocks annealing of complementary single-stranded DNA in a sequence-selective manner. Sci Rep. 4, 5464.
Lu, S., Edwards, M.C., 2016. Genome-wide analysis of small secreted cysteine-rich proteins identifies candidate effector proteins potentially involved in *Fusarium graminearum*-wheat interactions. Phytopathology 106, 166–176.
Lu, S., Edwards, M.C., 2018. Molecular characterization and functional analysis of PR-1-like proteins identified from the wheat head blight fungus *Fusarium graminearum*. Phytopathology 108, 510–520.
Lu, S., Faris, J.D., Edwards, M.C., 2017. Molecular cloning and characterization of two novel genes from hexaploid wheat that encode double PR-1 domains coupled with a receptor-like protein kinase. Mol. Genet. Genom. 292, 435–452.
Lu, S., Faris, J.D., Edwards, M.C., 2018. Molecular cloning and comparative analysis of a *PR-1-RK* hybrid gene from *Triticum urartu*, the A-genome progenitor of hexaploid wheat. Plant Mol. Biol. Reporter. 36, 469–483.
Lu, S., Faris, J.D., Sherwood, R., Edwards, M.C., 2013. Dimerization and protease resistance: new insight into the function of PR-1. J. Plant Physiol. 170, 105–110.
Lu, S., Lyngholm, L., Yang, G., Bronson, C., Yoder, O.C., Turgeon, B.G., 1994. Tagged mutations at the Tox1 locus of *Cochliobolus heterostrophus* by restriction enzyme-mediated integration. Proc. Natl. Acad. Sci. USA 91, 12649–12653.
Lu, S.W., Kroken, S., Lee, B.N., Robbertse, B., Churchill, A.C., Yoder, O.C., Turgeon, B.G., 2003. A novel class of gene controlling virulence in plant pathogenic ascomycete fungi. Proc. Natl. Acad. Sci. USA 100, 5980–5985.
Marchler-Bauer, A., Bo, Y., Han, L., He, J., Lanczycki, C.J., Lu, S., Chitsaz, F., Derbyshire, M.K., Geer, R.C., Gonzales, N.R., Gwadz, M., Hurwitz, D.I., Lu, F., Marchler, G.H., Song, J.S., Thanki, N., Wang, Z., Yamashita, R.A., Zhang, D., Zheng, C., Geer, L.Y., Bryant, S.H., 2017. CDD/SPARCLE: functional classification of proteins via subfamily domain architectures. Nucleic Acids Res. 45, D200–D203.
McMullen, M., Jones, R., Gallenberg, D., 1997. Scab of wheat and barley: a re-emerging disease of devastating impact. Plant Dis. 81, 1340–1348.
Oliver, R.P., Friesen, T.L., Faris, J.D., Solomon, P.S., 2012. *Stagonospora nodorum*: from pathology to genomics and host resistance. Annu. Rev. Phytopathol. 50, 23–43.
Park, C.M., Bruenn, J.A., Ganesa, C., Flurkey, W.F., Bozarth, R.F., Koltin, Y., 1994. Structure and heterologous expression of the *Ustilago maydis* viral toxin KP4. Mol. Microbiol. 11, 155–164.
Proctor, R.H., Hohn, T.M., McCormick, S.P., 1995. Reduced virulence of *Gibberella zeae* caused by disruption of a trichothecene toxin biosynthetic gene. Mol. Plant Microbe Interact. 8, 593–601.
Quijano, C.D., Wichmann, F., Schlaich, T., Fammartino, A., Huckauf, J., Schmidt, K., Unger, C., Broer, I., Sautter, C., 2016. KP4 to control *Ustilago tritici* in wheat: enhanced greenhouse resistance to loose smut and changes in transcript abundance of pathogen related genes in infected KP4 plants. Biotechnol. Rep. (Amst) 11, 90–98.
Roncero, M.I.G., Hera, C., Ruiz-Rubio, M., Maceira, F.I.G., Madrid, M.P., Caracuel, Z.,

Calero, F., Delgado-Jarana, J., Roldán-Rodrıguez, R., Martınez-Rocha, A.L., Velasco, C., Roa, J., Martın-Urdiroz, M., Córdoba, D., Di Pietro, A., 2003. *Fusarium* as a model for studying virulence in soilborne plant pathogens. Physiol. Mol. Plant Pathol. 62, 87–98.

Shaner, G.E., Epidemiology of Fusarium head blight of small grain cereals in North America. In: Leonard, K.J., Bushnell, W.R. (Eds.), Fusarium head blight of wheat and barley. The American Phytopathological Society Press. pp 84–119, St. Paul, MN, 2003, pp. 84–119.

Stephens, A.E., Gardiner, D.M., White, R.G., Munn, A.L., Manners, J.M., 2008. Phases of infection and gene expression of *Fusarium graminearum* during crown rot disease of wheat. Mol. Plant Microbe Interact. 21, 1571–1581.

Thompson, J.D., Gibson, T.J., Plewniak, F., Jeanmougin, F., Higgins, D.G., 1997. The CLUSTAL_X windows interface: flexible strategies for multiple sequence alignment aided by quality analysis tools. Nucleic Acids Res. 25, 4876–4882.

Turgeon, B.G., Condon, B., Liu, J., Zhang, N., 2010. Protoplast transformation of filamentous fungi. Methods Mol. Biol. 638, 3–19.

Voigt, C.A., Schafer, W., Salomon, S., 2005. A secreted lipase of F*usarium graminearum* is a virulence factor required for infection of cereals. Plant J. 42, 364–375.

Wang, Q., Shao, B., Shaikh, F.I., Friedt, W., Gottwald, S., 2018. Wheat resistances to Fusarium root rot and head blight are both associated with deoxynivalenol- and jasmonate-related gene expression. Phytopathology 108, 602–616.

Wang, Q., Vera Buxa, S., Furch, A., Friedt, W., Gottwald, S., 2015. Insights into *Triticum aestivum* seedling root rot caused by *Fusarium graminearum*. Mol. Plant Microbe Interact. 28, 1288–1303.

Wang, Y.J., Yu, J.N., Chen, T., Zhang, Z.G., Hao, Y.J., Zhang, J.S., Chen, S.Y., 2005. Functional analysis of a putative Ca^{2+} channel gene TaTPC1 from wheat. J. Exp. Bot. 56, 3051–3060.

White, P.J., Broadley, M.R., 2003. Calcium in plants. Ann. Bot. 92, 487–511.

Zhang, Y.Z., Chen, Q., Liu, C.H., Liu, Y.B., Yi, P., Niu, K.X., Wang, Y.Q., Wang, A.Q., Yu, H.Y., Pu, Z.E., Jiang, Q.T., Wei, Y.M., Qi, P.F., Zheng, Y.L., 2016. Chitin synthase gene FgCHS8 affects virulence and fungal cell wall sensitivity to environmental stress in *Fusarium graminearum*. Fungal Biol. 120, 764–774.